TAYLOR-COUETTE-POISEUILLE FLOWS : FROM RANS TO LES

Christophe Friess, Sébastien Poncet, Stéphane Viazzo

International Symposium
On Turbulence and Shear Flow
Phenomena (TSFP-8)
August 28 - 30, 2013 Poitiers, France

TAYLOR-COUETTE-POISEUILLE FLOWS : FROM RANS TO LES

Christophe Friess, Sébastien Poncet and Stéphane Viazzo
Laboratoire M2P2, UMR CNRS 7340
Aix-Marseille Université / CNRS
38, rue Frédéric Joliot-Curie
13451 MARSEILLE Cedex 13
friess@l3m.univ-mrs.fr

ABSTRACT

The present paper proposes a study of a Taylor-Couette-Poiseuille flow in a narrow gap between a rotor and a stator, using two different rotation rates. Refined Large-Eddy Simulation results, using the WALE model Nicoud & Ducros (1999), hold for reference data, whereas the efficiency of a RANS model, the Elliptic Blending Reynolds Stress Model (EB-RSM) (Manceau & Hanjalić, 2002; Manceau, 2005), and a hybrid RANS/LES method, the so-called "Equivalent DES" (Manceau *et al.*, 2010; Friess & Manceau, 2012) is studied.

INTRODUCTION

Since Taylor's first theoretical results obtained one century ago, researchers have dedicated obstinate efforts in modelling the rich dynamical behaviour exhibited by the flow moving between two concentric cylinders in differential rotation. In spite of the substantial literature on flows through rotating concentric annuli, little is known about the near-wall turbulent structures in such systems. This kind of flow is often encountered in turbomachinery. In addition, it provides also insights into the general problem of three-dimensional turbulent boundary layers. The combined axial and rotational flow in an annulus was studied experimentally by Escudier & Gouldson (1995). Most numerical studies until now used turbulence modelling, which provided rather limited informations. It was shown that increasing the rotation rate of the inner tube amplified the turbulent kinetic energy, resulting in the enhancement of heat transfer (Poncet *et al.*, 2011; Rothe & Pfitzer, 1997). The development of computational methods (including Direct and Large Eddy Simulations) has led to an increase in numerical studies of rotating flows, but little concern turbulent Taylor-Couette-Poiseuille flows. As example, Chung & Sung (2005) established the destabilization of the near-wall turbulent structures due to rotation of the inner wall giving rise to an increase of sweep and ejection events. Compared to this latter, we focus our attention here on the narrow gap case, which models quite faithfully flows in the rotor-stator gap of electrical motors.
The aim of the present work is twofold : (i) providing some reference LES data for this case, using an in-house code and (ii) questioning the capabilities of a hybrid RANS / LES method, as well as the underlying RANS model, in predicting this kind of flow.

FLOW CONFIGURATION AND PARAMETERS

The fluid is confined between two concentric cylinders of radii R_1 and R_2 and of height h (see Figure 1). The inner cylinder represents a rotor, thus rotating at a constant rate Ω, while the outer one is stationary. The cavity may be characterized by two geometrical parameters : its aspect ratio $\Gamma = h/(R_2 - R_1)$ and its radius ratio $\eta = R_1/R_2$. An axial throughflow is imposed within the gap at a constant bulk velocity W_m. The main flow parameters are the rotational Reynolds number $Re_\Omega = \Omega R_1(R_2 - R_1)/\nu$ and the bulk Reynolds number $Re_Q = W_m(R_2 - R_1)/\nu$, ν being the fluid's kinematic viscosity. The present study considers two values of the ratio $N = Re_\Omega/Re_Q$ (see Table 1), while other parameters remain unchanged.

Case	A	B
Γ	10	10
η	8/9	8/9
Re_Q	3745	3745
N	2.24	4.47

Table 1. Geometrical and flow parameters for the two cases

NUMERICAL METHODS

Concerning LES reference calculations, the numerical method of the in-house code is based on the work of Abide & Viazzo (2005), which devised a 2D compact fourth-order projection decomposition method in cartesian coordinates. It has been recently validated in the case of turbulent inter-disk rotor-stator flows in cylindrical coordinates by Viazzo *et al.* (2012) but also for turbulent Taylor-Couette-Poiseuille flows in a middle gap cavity (Oguic *et al.*, 2013). The time advancement is second order accurate and is based on the explicit Adams-Bashforth scheme for the convective terms and an implicit backward Euler scheme for the viscous terms. The derivatives are approximated using fourth order compact formula in the radial and axial directions. The time splitting scheme is an improved projection method, which ensures the incompressibility at each time step. The

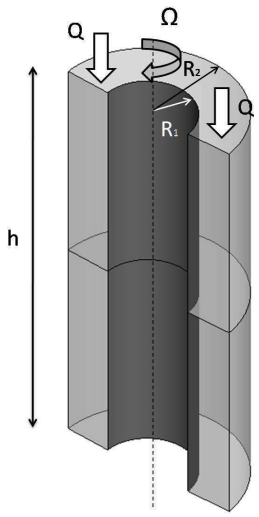

Figure 1. Sketch of the narrow gap cavity

projection decomposition method is based on a direct non-overlapping multidomain Helmholtz/Poisson solver, which provides the solution of each Helmholtz/Poisson problem resulting of the velocity-pressure coupling. The multidomain solver ensures the continuity of the solution and its first normal derivative across the conforming interface. These continuity conditions are cleared up using an influence matrix technique. By assuming the periodicity of the solution in the azimuthal direction, the three-dimensional extension uses Fourier series. The set of problems is thus reduced to a series of two-dimensional problems associated with each wave number. Periodic boundary conditions are applied in the axial and circumferential (angle of $3\pi/4$) directions and no-slip boundary conditions are imposed on the walls. The LES grid contains $65 \times 144 \times 130$ points respectively in the radial, azimuthal and axial directions.

The CFD code used for RANS and hybrid RANS/LES simulations is the open-source *Code_Saturne*, developped by EDF (Archambeau *et al.*, 2004). It is a finite volume solver, written in cartesian coordinates. A SIMPLEC algorithm, with the Rhie and Chow interpolation, is used for pressure-velocity coupling.

Concerning hybrid RANS/LES calculations, convective fluxes are approximated by a second-order centered scheme, for momentum, and a first-order upwind scheme for subfilter quantities. Time marching uses a Crank-Nicholson, second order scheme. The hybrid RANS/LES mesh contains 60^3 cells, with an angular periodicity of $\pi/2$ and an axial periodicity. No-slip boundary conditions are imposed on the walls. The RANS mesh is a 1D grid of 60 cells. In RANS mode, convective fluxes are approximated by a first-order upwind scheme, for all computed quantities, and the time scheme is first order.

TURBULENCE MODELLING

Various levels of modelling are presented. Emphasis is first put on the hybrid RANS/LES method. Afterwards, the subfilter closure and RANS model will be briefly presented.

Hybrid method

The hybrid method used for the present work is the "Equivalent DES" of (Manceau *et al.*, 2010; Friess & Manceau, 2012). This approach was first derived for the purpose of bridging the PITM (Partially Integrated Transport Model) (Chaouat & Schiestel, 2005) and the DES (Detached Eddy Simulation) method. Indeed, the first is fully justified from a theoretical point of view, while the second one was developped on a rather phenomenological basis. First, the PITM was generalized by Fadai-Ghotbi *et al.* (2010*b*) to inhomogeneous flows, considering temporal filtering, rather than spatial filtering. Indeed, inhomogeneous flows are more frequent. Since, in this kind of flow, the RANS operator corresponds, by ergodicity, to temporal averaging. Since any seamless (continuously transitioning) RANS/LES method must tend to RANS, at large filter width, inhomogeneous flow studies need then to consider hybrid RANS / temporal LES. Nevertheless, from a pragmatical point of view, considering RANS / TLES hybridization does not cause any difficulty in implementing models or special terms, since Fadai-Ghotbi *et al.* (2010*b*) showed that applying Temporal PITM (T-PITM) to a inhomogeneous stationary flow is just equivalent to applying PITM to homogeneous, statistically unsteady flow. Actually, one must just keep in mind that "hybrid RANS/LES" is to be understood in a general way, including temporal LES.

The advantage of Detached Eddy Simulation lies in its simplicity and robustness. The idea of Manceau *et al.* (2010) was thus to derive an approach bridging it with T-PITM. This latter is, in spite of its theoretical justification, not very easy to implement in any code, showing some numerical issues. An equivalence criterion was then determined between T-PITM and DES, providing some theoretical justification to the latter, and allowing to interprete it as a hybrid RANS / temporal LES method. This equivalence criterion was derived analytically for equilibrium flows, but was successfully tested on a flow over a periodic hill, involving massive separation (Friess & Manceau, 2012).

The principle of DES is to magnify the dissipation term of the transport equation for either subfilter turbulent kinetic k_{SFS} energy or subfilter stresses $\tau_{ij_{SFS}}$, damping the modelled energy and allowing large scale eddies to be resolved:

$$\varepsilon_{ij}^{DES} = \frac{k_{SFS}^{3/2}}{\varepsilon_{SFS} L} \varepsilon_{ij_{SFS}} \,. \tag{1}$$

While classical DES uses the local grid step to determine the length scale L in (1), equivalent DES uses the ratio r defined as :

$$r = \frac{k_m}{k} \,, \tag{2}$$

where k is the total turbulent kinetic energy, and k_m its counterpart contained in the modelled (subfilter) scales. At the RANS limit, r tends to 1, and at the DNS limit, it tends to 0. The advantage of r is that it can be estimated using a spatial or a temporal energy spectrum. As shown by Friess & Manceau (2012), r can be evaluated as :

$$\begin{aligned} r &= \frac{1}{k} \int_{\omega_c}^{\infty} E_T(\omega)\, d\omega \\ &= \min\left(1, \frac{1}{\beta_0} \left(\frac{U_s}{\sqrt{k}}\right)^{2/3} \left(\omega_c \frac{k}{\varepsilon}\right)^{-2/3}\right). \end{aligned} \tag{3}$$

β_0 being a constant derived from the Kolmogorov constant (we used 0.3 here), U_S a sweeping velocity and ω_c the cutoff frequency of the considered filter. It can be defined as :

$$\omega_c = \min\left(\frac{\pi}{\mathrm{dt}}; \frac{U_s \pi}{\Delta}\right) , \tag{4}$$

where dt and Δ are the time and grid steps, respectively. Finally, following Manceau *et al.* (2010), the length scale L entering (1) is :

$$L = \frac{r^{3/2}}{1 + \frac{C_{\varepsilon 2} - C_{\varepsilon 1}}{C_{\varepsilon 1}}(1 - r^{C_{\varepsilon 1}/C_{\varepsilon 2}})} \frac{k^{3/2}}{\varepsilon} , \tag{5}$$

RANS model and subfilter closure

In the temporally-filtered Navier-Stokes equation, the subfilter stresses must be modeled such a way that, making the temporal filter width go to infinity, the equations tend to the RANS equations. In particular, one of the main objectives of hybrid methods is to use RANS closures in the near-wall regions, to avoid the very fine resolution required by LES. In that aim, the RANS model proposed by Manceau & Hanjalić (2002) and Manceau (2005), the so-called *elliptic blending Reynolds-Stress Model* (EB-RSM), is adapted to the hybrid temporal LES context. In this model, an elliptic relaxation equation is solved for a scalar α :

$$\alpha - L_{SFS}^2 \nabla^2 \alpha = 1 , \tag{6}$$

which is a sensor of the distance to the wall ($\alpha = 0$ at the wall, and 1 far away), and is used to blend near-wall and homogeneous formulations for the redistribution and dissipation terms of the transport equations for subfilter stresses (see Fadai-Ghotbi *et al.* (2010*a*) for details) :

$$\phi_{ij}^* - \varepsilon_{ij} = \alpha^3 (\phi_{ij}^* - \varepsilon_{ij})_{\text{wall}} + (1 - \alpha^3)(\phi_{ij}^* - \varepsilon_{ij})_{\text{homogeneous}} . \tag{7}$$

Under its RANS form, EB-RSM was successfully applied to several flows, such as non-rotating and rotating channels (Manceau, 2005), impinging jets (Thielen *et al.*, 2005) or mixed and natural convection flows (Dehoux *et al.*, 2011). It was recently adapted by Fadai-Ghotbi *et al.* (2010*a*) to serve as a subfilter-stress model in the framework of T-PITM. In the present work, it is also applied as a model for the equivalent DES, by simply substituting the dissipation in the fashion of Eq. (1) in the Reynolds-stress transport equations.

Subgrid-scale model

Eventually, LES calculations were performed using the Wall-Adapting Local Eddy Viscosity (WALE) model of Nicoud & Ducros (1999). This choice was motivated by a better numerical stability than the dynamic Smagorinsky model, and its quality in near-wall treatment without damping functions. The subgrid viscosity is given by :

$$\nu_t = (C_w \Delta)^2 \frac{(S_{ij}^d S_{ij}^d)^{3/2}}{(\overline{S}_{ij}\overline{S}_{ij})^{5/2} + (S_{ij}^d S_{ij}^d)^{5/4}} , \tag{8}$$

where C_w is a constant, Δ the grid step, $\overline{S}_{ij}$ the filtered strain-rate tensor, and S_{ij}^d the deviatoric part of the squared filtered velocity gradient tensor.

RESULTS AND DISCUSSION

Hereafter, some sample results are shown. Both rotation rates are represented on same graphs, in order to show the influence of N. Comparison between the reference LES, hybrid RANS/LES and RANS is proposed.

Velocity profiles are first presented on Figure 2. Good agreement is observed, especially inside boundary layers, as expected, since near-wall treatment without empirical laws is a feature of EB-RSM. On the contrary, the classical turbulent Poiseuille profile observed for the axial velocity is not captured by the hybrid approach, which is not surprising (see e.g. Fadai-Ghotbi *et al.* (2010*a*)). At $N = 2.24$, the slope of azimuthal velocity V_θ is also particularly badly predicted by RANS and hybrid RANS/LES in the free flow. Figures 3 and 4 show the normal and shear components of the Reynolds stress tensor. As expected, $R_{\theta\theta}$ increases strongly with N, as well as $R_{\theta r}$ and $R_{\theta z}$ shear stresses intensities. Other components increase in a more marginal way, only due to redistribution. Another interesting feature, is that all components are far more symmetric than in the middle-gap (η = 0.5) studied by Oguic *et al.* (2013), confirming that the flow field near the stator side is significantly influenced by the motion of the rotor, especially at those quite high values of N. Predictions by both RANS and hybrid RANS/LES approaches do not show clear hierarchy between them, but nevertheless RANS seems more efficient than hybrid RANS/LES for $N = 2.24$, and vice-versa for $N = 4.47$. Peak locations and especially intensities are not very well reproduced, but in a quite satisfactory way. This is the cause for the weak prediction of velocity profiles in the free flow, evoked above.

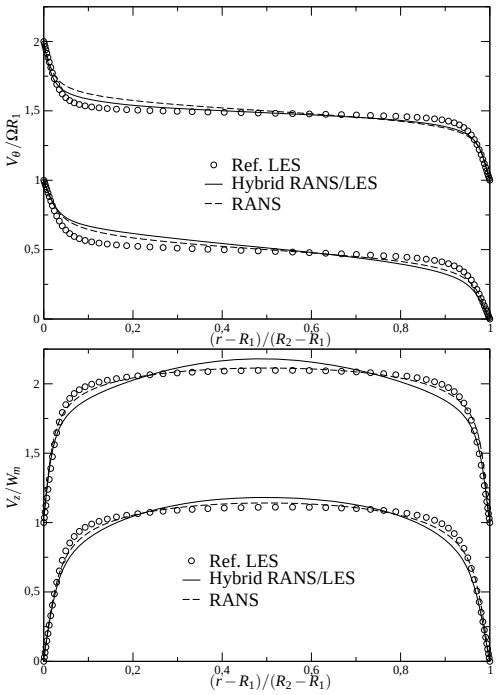

Figure 2. Azimuthal and axial velocity profiles, for both rotation rates. Profiles for N=4.47 are shifted up, for clarity.

Figure 5 compares observed and targetted values of the energy ratio r. "Targetted" means that r is evaluated by Eq. (3), while "observed" refers to post-processed r, in the fashion of Eq. (2), requiring to compute the modelled k_m and the

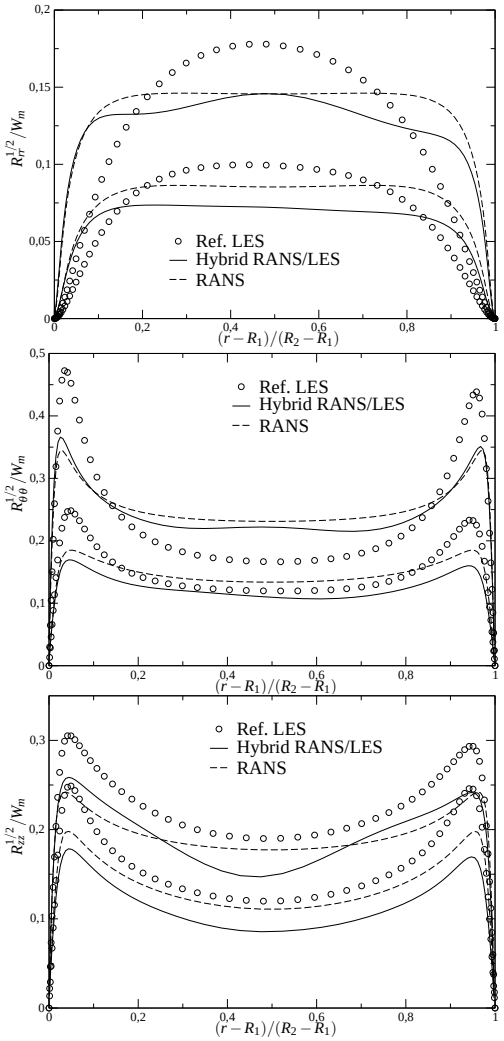

Figure 3. Root mean square velocities, for both rotation rates. Higher curves correspond to N=4.47.

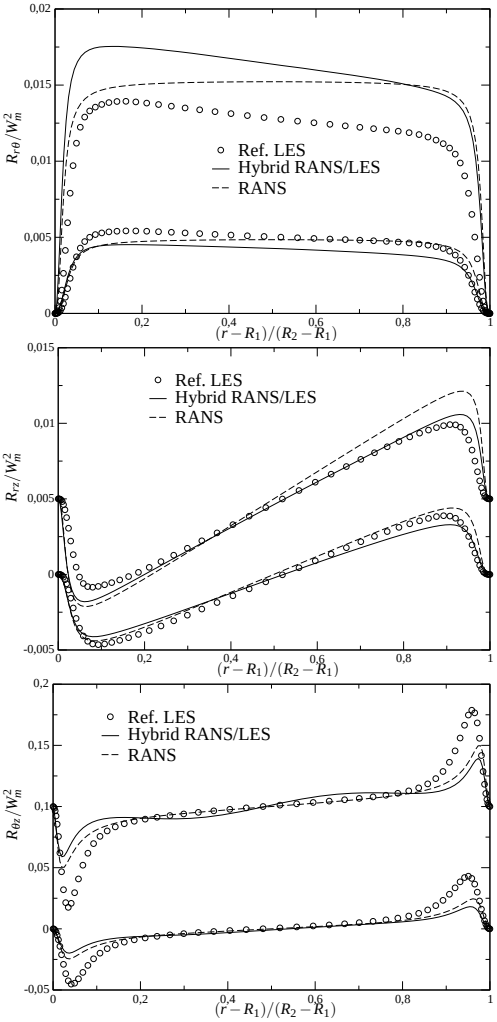

Figure 4. Shear components of the Reynolds stress tensor for both rotation rates. Profiles for N=4.47 are shifted up, for clarity.

resolved k_{res} parts of the turbulent kinetic energy. For the same mesh, it seems that r is globally lower at $N = 4.47$ than at $N = 2.24$, which may explain why hybrid RANS/LES predictions are slightly better than RANS at $N = 4.47$, since the level of explicitly resolved energy is then bigger. Note that RANS mode $r = 1$ is enforced near walls, in order to allow EB-RSM to fully play its role. Nevertheless, the observed ratio does not obey it exactly. Indeed, the outer flow fluctuations influence the behaviour even inside the viscous sublayer.

Figures 6 and 7 show isocontours of arbitrary Q-criterion values, seen from the rotor side. Obviously, the LES simulations show far more structures than hybrid RANS/LES ones. Nevertheless, an interesting behaviour is exhibited by both approaches : the streaks form a kind of net, because of the significant bidimensionality of the flow, and this net's angle changes with N, tending to place the main structures in the (r, θ) plane.

Eventually, Table 2 summarizes the wall quantities and numerical resolutions in wall units, for all approaches. While good global agreement is found for Re_τ at $N = 2.24$, there is more dispersion at $N = 4.47$, especially at the inner wall. Another interesting observation, is that Re_τ is always equal at the inner and the outer walls, because the velocity gradient is the same at both walls.

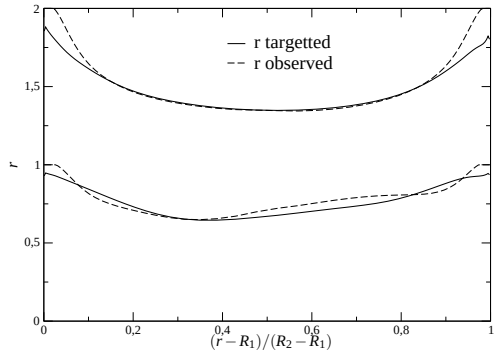

Figure 5. Targetted and observed values of the energy ratio r, for both rotation rates. Profiles for N=4.47 are shifted up, for clarity.

SUMMARY

The present work is a first step in numerical simulation of Taylor-Couette-Poiseuille flows in narrow rotor-stator cavities.
Assuming that Large Eddy Simulation results can be considered as reference as this approach has been already validated in a middle gap cavity Oguic *et al.* (2013), it seems

N	2.24			4.47		
method	LES	HRLES	RANS	LES	HRLES	RANS
r_i^+	0.46	0.50	0.51	0.65	0.83	0.73
r_o^+	0.42	0.46	0.51	0.59	0.73	0.73
$(R_1\Delta\theta)^+$	44.3	69.3	-	62.5	114.2	-
$(R_2\Delta\theta)^+$	45.4	70.6	-	63.0	113.4	-
Δz_i^+	26	55.1	-	36.7	90.9	-
Δz_o^+	23.7	49.9	-	32.9	80.2	-
$Re_{\tau,i}$	338	331	333	477	545	483
$Re_{\tau,o}$	308	300	333	428	481	483

Table 2. Wall resolution and mean flow parameters.

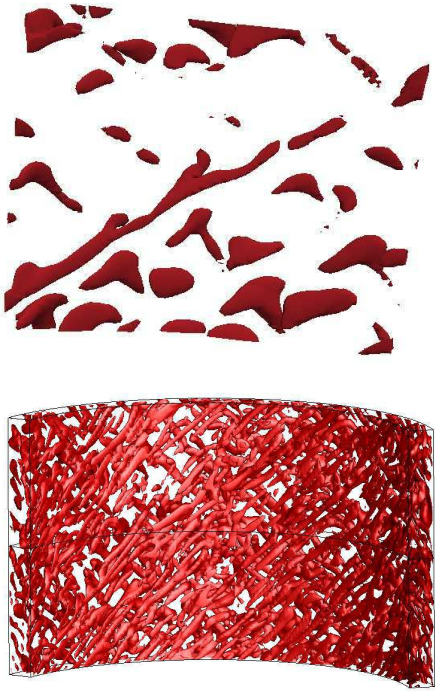

Figure 6. Isocontours of Q-criterion (arbitrary value), for N=2.24. Up : hybrid RANS/LES, down : reference LES

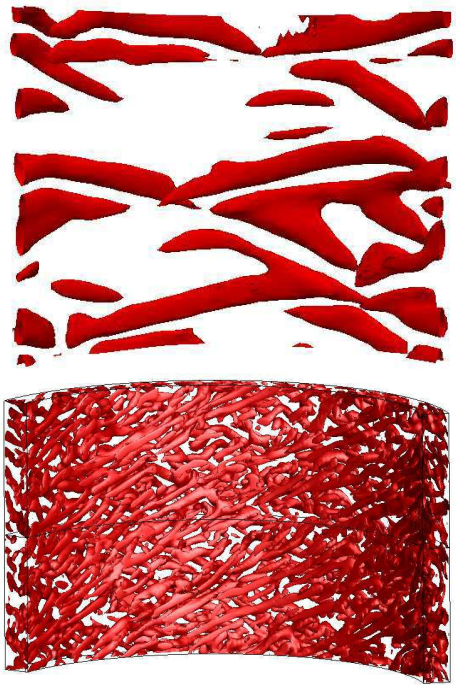

Figure 7. Isocontours of Q-criterion (arbitrary value), for N=4.47. Up : hybrid RANS/LES, down : reference LES

that the hybrid RANS/LES computation does not improve the mean prediction, in comparison with RANS. This tendency was also observed by Fadai-Ghotbi *et al.* (2010*a*) on a simple channel flow. However, Q-criterion observation, with hybrid RANS/LES, exhibits net-shaped streaks, as well as the changing of the angle of the main directions of this net. This configuration is also observed with LES, with obviously more details.
Besides a larger study on some other values of the axial Reynolds number and other rotation rates, a next step is accounting for heat transfer.

ACKNOWLEDGEMENTS

This work was financially supported by Liebherr Aerospace (project “Entrefer moteur”) and by the LABEX MEC (project “Hydrex”), which are gratefully acknowledged.

REFERENCES

Abide, S. & Viazzo, S. 2005 A 2D compact fourth-order projection decomposition method. *J. Comput. Phys.* **206**, 252–276.

Archambeau, F., Méchitoua, N. & Sakiz, M. 2004 Code Saturne: A finite volume code for the computation of turbulent incompressible flows - Industrial applications. *Int. J. on Finite Volume, Electronical edition: http://averoes.math.univ-paris13.fr/html* **ISSN 1634** (0655).

Chaouat, B. & Schiestel, R. 2005 A new partially integrated transport model for subgrid-scale stresses and dissipation rate for turbulent developing flows. *Phys. Fluids*

17 (065106), 1–19.

Chung, S.Y. & Sung, H.J. 2005 Large-eddy simulation of turbulent flow in a concentric annulus with rotation of an inner cylinder. *Int. J. Heat Fluid Flow* **26**, 191–203.

Dehoux, F., Benhamadouche, S. & Manceau, R. 2011 Modelling turbulent heat fluxes using the elliptic blending approach for natural convection. In *Proc. 7th Int. Symp. Turb. Shear Flow Phenomena, Ottawa, Canada*.

Escudier, M.P. & Gouldson, I.W. 1995 Concentric annular flow with centerbody rotation of a newtonian and a shear-thinning liquid. *Int. J. Heat Fluid Flow* **16**, 156–162.

Fadai-Ghotbi, A., Friess, C., Manceau, R. & Borée, J. 2010*a* A seamless hybrid RANS/LES model based on transport equations for the subgrid stresses and elliptic blending. *Phys. Fluids* **22**, 055104.

Fadai-Ghotbi, A., Friess, C., Manceau, R., Gatski, T.B. & Borée, J. 2010*b* Temporal filtering : A consistent formalism for seamless hybrid RANS/LES in inhomogeneous turbulence. *Int. J. Heat Fluid Flow* **31**, 378–389.

Friess, C. & Manceau, R. 2012 Investigation of the equivalence of two hybrid temporal-LES methods based on elliptic blending in separated flows. In *Proc. 7th Int. Symp. Turbulence, Heat and Mass Transfer, Palermo, Italy*.

Manceau, R. 2005 An improved version of the Elliptic Blending Model. Application to non-rotating and rotating channel flows. In *Proc. 4th Int. Symp. Turb. Shear Flow Phenomena, Williamsburg, VA, USA*.

Manceau, R., Friess, C. & Gatski, T.B. 2010 Of the interpretation of DES as a hybrid RANS / temporal LES method. In *8th ERCOFTAC Int. Symposium on Engineering Turbulence Modelling and Measurements, Marseille, France*.

Manceau, R. & Hanjalić, K. 2002 Elliptic blending model: A new near-wall Reynolds-stress turbulence closure. *Phys. Fluids* **14** (2), 744–754.

Nicoud, F. & Ducros, F. 1999 Subgrid-scale stress modelling based on the square of the velocity gradient tensor. *Flow, Turb. and Comb.* **62**, 183–200.

Oguic, R., Viazzo, S. & Poncet, S. 2013 Numerical simulations of a middle gap turbulent Taylor-Couette-Poiseuille flow. In *Direct and Large-Eddy Simulation 9*. Dresden.

Poncet, S., Haddadi, S. & Viazzo, S. 2011 Numerical modeling of fluid flow and heat transfer in a narrow Taylor-Couette-Poiseuille system. *Int. J. Heat Fluid Flow* **32**, 128–144.

Rothe, T. & Pfitzer, H. 1997 The influence of rotation on turbulent flow and heat transfer in an annulus between independently rotating tubes. *Int. J. Heat and Mass Transfer* **32**, 353–364.

Thielen, L., Hanjalić, K., Jonker, H. & Manceau, R. 2005 Predictions of flow and heat transfer in multiple impinging jets with an elliptic-blending second-moment closure. *Int. J. Heat and Mass Transfer* **48** (8), 1583–1598.

Viazzo, S., Poncet, S., Serre, E., A., Randriamampianina & Bontoux, P. 2012 High-order Large Eddy Simulations of confined rotor-stator flows. *Flow, Turb. and Comb.* **88 (1-2)**, 63–75.